LETTERS

Global electromagnetic induction constraints on transition-zone water content variations

Anna Kelbert[1], Adam Schultz[1] & Gary Egbert[1]

Small amounts of water can significantly affect the physical properties of mantle materials, including lowering of the solidus[1], and reducing effective viscosity[2] and seismic velocity[3]. The amount and distribution of water within the mantle thus has profound implications for the dynamics and geochemical evolution of the Earth[4,5]. Electrical conductivity is also highly sensitive to the presence of hydrogen in mantle minerals[6]. The mantle transition zone minerals wadsleyite and ringwoodite in particular have high water solubility[4], and recent high pressure experiments show that the electrical conductivity of these minerals is very sensitive to water content[7–9]. Thus estimates of the electrical conductivity of the mantle transition zone derived from electromagnetic induction studies have the potential to constrain the water content of this region. Here we invert long period geomagnetic response functions to derive a global-scale three-dimensional model of electrical conductivity variations in the Earth's mantle, revealing variations in the electrical conductivity of the transition zone of approximately one order of magnitude. Conductivities are high in cold, seismically fast, areas where slabs have subducted into or through the transition zone. Significant variations in water content throughout the transition zone provide a plausible explanation for the observed patterns. Our results support the view[10,11] that at least some of the water in the transition zone has been carried into that region by cold subducting slabs.

Electromagnetic induction sounding of the Earth's mantle entails inverting impedance functions calculated from the ratios of magnetic (geomagnetic depth sounding) or electric and magnetic (magnetotelluric) field components. Magnetic variations with periods of approximately 2–100 days, which are associated with the relaxation phase of disturbed storm time (D_{st}) variations of the magnetospheric equatorial ring current, provide good resolution in and just below the mantle transition zone[12]. Until recently, the principal constraints on electrical conductivity at these depths have derived from one-dimensional inversion of geomagnetic depth sounding and/or magnetotelluric responses (Methods). Several recent studies have discussed significant spatial variability in transition-zone electrical conductivity, and its implications for water content[13,14], but these have all been based on one-dimensional local interpretations. Regional magnetotelluric surveys, which are generally interpreted with two-dimensional models, typically extend to periods of no longer than 10^4 s (10^5 s for seafloor magnetotellurics), thus essentially limiting studies to the upper mantle and top of the transition zone[15]. Initial efforts at three-dimensional inversion of very long period geomagnetic depth sounding and magnetotelluric data, including a regional model of the North Pacific[16,17] and a global-scale inversion using an approximate forward modelling scheme[18], have so far provided very limited views of whole mantle conductivity.

To obtain a global three-dimensional model of mantle electrical conductivity, we use a frequency-domain, regularized nonlinear conjugate gradient inversion for the spherical Earth[12]. We parameterize the electrical conductivity in the mantle (depths of 12.65–1,600 km) by a series of spherical shells, in each of which lateral conductivity variations about a one-dimensional prior model[19] are represented by a spherical harmonic expansion of degree and order nine. The prior model has been discretized into 12 layers[12], allowing for conductivity jumps at 410, 520 and 670 km depths, related to the major mineral phase transitions. The lower four layers (1,600 km and deeper) were constrained to be homogeneous. The inversions were regularized by minimizing deviations from the prior model, with a norm that penalized higher degree and order terms, and jumps between layers. For our study, we have used a compilation of 59 observatories equator-ward of 60° geomagnetic latitude from global observatory data sets[20,21]. Responses at 28 periods from 5 to 106.7 days were inverted (Methods Summary).

An extensive set of computational experiments were performed, using different combinations of vertical and horizontal regularizations, damping parameters, and degrees and orders of spherical harmonic model parameterization, with the effect of isolated or possibly anomalous observatories tested by omitting these from the inversion. The large-scale pattern of mid-mantle heterogeneities that emerges from all of these tests is robust, although details of the locations of boundaries between regions of differing conductivity, as well as the amplitudes of the heterogeneities, vary somewhat. We have also explored the trade-off between data fit and model norm. The full data set can be fitted to a normalized root mean square (r.m.s.) of 1.06, only slightly larger than the idealized target normalized r.m.s. of 1. Bearing in mind that modelling inaccuracies and source complications are not accounted for in the statistical data error estimates, we choose a slightly poorer fitting (r.m.s. = 1.14) model for further discussion (Fig. 1). Better fitting models exhibit similar spatial structure, but with larger amplitude anomalies.

The pattern of lateral heterogeneities in our models appears continuous through and below the mantle transition zone. This may result from the limited vertical resolution of this data set, and the regularization employed. The induction data cannot distinguish between a thin layer of very high conductivity at the base of the transition zone and more moderate conductivities spreading into the lower mantle. Inversion of synthetic data with an identical distribution of sites and comparable signal and noise characteristics demonstrates[12] that in regions with good data coverage, large-scale structures at depths of ~500–1,600 km are resolved relatively well, even if shorter wavelength conductivity variations are present. However, the deeper structures should be interpreted with some caution owing to possible distortion or masking by the high electrical conductivities of the transition zone. Here we focus on the structure in, and just below, the transition zone (depths <900 km). In regions with poor data coverage, including most of Africa, South America, and the Indian and South Pacific Oceans, conductivity is poorly constrained at all mantle depths[12].

[1]College of Oceanic & Atmospheric Sciences, Oregon State University, Corvallis, Oregon 97331-5503, USA.

410–520

900–1,200

520–670

1,200–1,600

670–900

$\log_{10}(\sigma)$
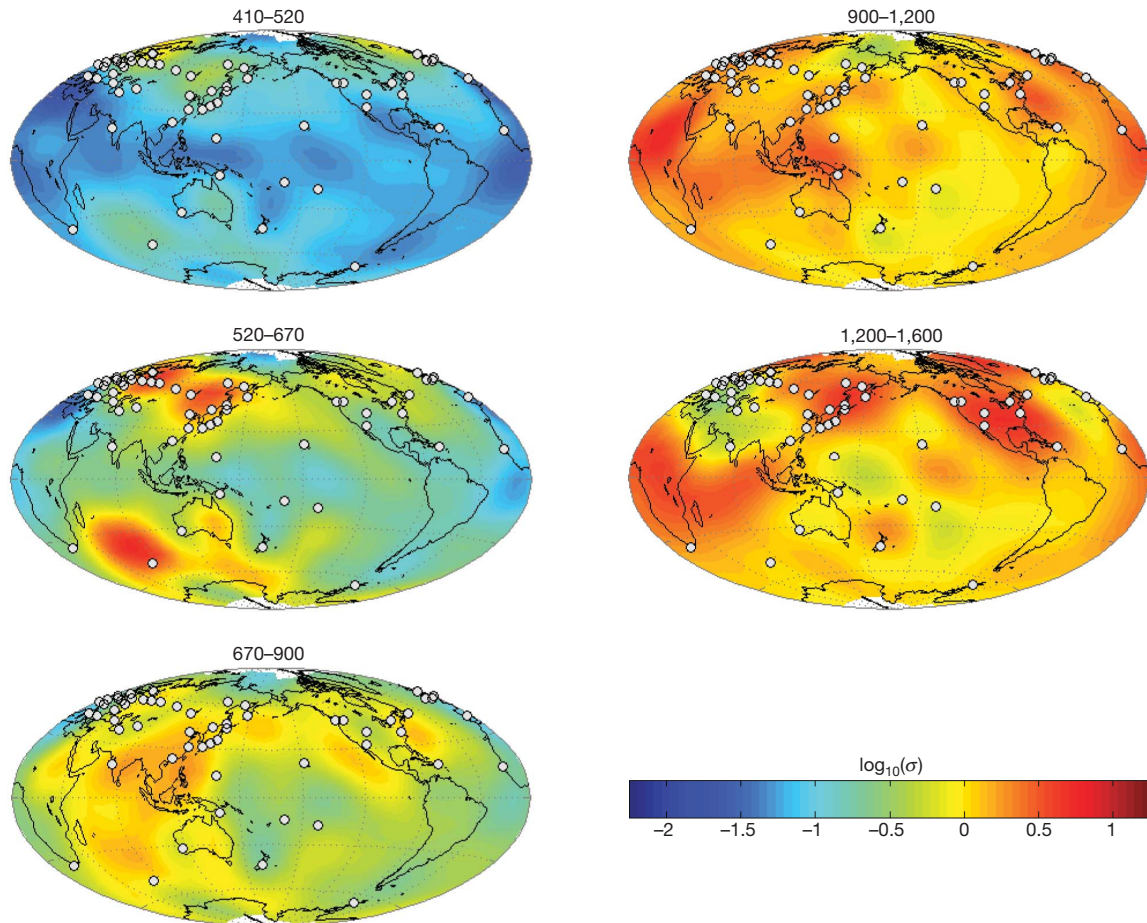
−2   −1.5   −1   −0.5   0   0.5   1

Figure 1 | Regularized degree and order nine electrical conductivity inverse solution. The solution has been obtained by applying a global inversion algorithm[12] to C responses from the mid-latitude subset of the global observatory data set[20], supplemented by six C responses from ref. 21, with correction for near-surface effects[30]. Here, σ stands for electrical conductivity. The 59 data locations are denoted by white dots; the depths from the Earth's surface are indicated in km. The normalized r.m.s. misfit of this model is 1.14. Regions of poor spatial resolving power include most of Africa and the Indian Ocean, the Southern Pacific and South America.

The most notable feature in Fig. 1 at transition-zone depths is a band of enhanced conductivity along the circum-Pacific margin, extending from western North America, through the Aleutian arc and East Asia, and into the Indian Ocean and Australia. Most notably, high conductivity is registered beneath Japan, eastern China, and in the areas of the Izu-Bonin and Tonga slabs. The central Pacific basin is more than an order of magnitude more resistive than the surrounding conductive regions. Lack of continuity of this conductive feature, and its absence from the remaining parts of the circum-Pacific margin (for example, beneath South America) may be the result of the significant gaps in data coverage. The high conductivity areas in and below the mantle transition zone correlate well with the present-day distribution of cold, and seismically fast, subducted slabs[22], at least in areas with good model resolution. We also note positive correlation with maps of transition-zone thickness, and depth to the 410 km discontinuity[23].

These correlations strongly suggest that the high conductivities at transition-zone depths are linked to subducted oceanic lithosphere. Based on temperature alone, this cold subducted material should be relatively resistive[7,8]. Water, carried into the transition zone with the subducting slabs, provides a plausible explanation for the elevated conductivities. Transition-zone minerals have high water solubility[4] (about 2 wt%), and 1 wt% water raises the conductivity of dry wadsleyite and ringwoodite by more than an order of magnitude[7–9]. Water may also elevate conductivity indirectly by inducing melting in or immediately above or below the transition zone[5,14]. Oxidized carbon may also have a role in enhancing mantle conductivity (by inducing partial melt or otherwise), although evidence to date suggests[24] that such enhancements would be restricted to shallow transition-zone depths or above (Methods). Elevated iron content[25] would also increase conductivity of these transition-zone minerals.

The water content of the mantle transition zone may be roughly estimated using high-pressure laboratory measurements of electrical conductivity in samples of the transition-zone minerals of varying hydrogen content[7–9]. In Fig. 2, we compare electrical conductivity profiles from our three-dimensional inverse solution to those derived from the relation between conductivity and water content given in ref. 8, with water content varying from 0 to 1 wt%. Assuming the results of ref. 8, 0.5–1 wt% water might be required to achieve the highest conductivities in the lower transition zone (0.5–2.0 S m^{-1}, for example, beneath northeastern China and Japan), while the more resistive areas are consistent with dry mantle conditions, with no more than 0.1 wt% water. Slightly lower water content would be inferred in the conductive anomalies from the results of ref. 9. More rigorous quantification of water content must await resolution of uncertainties in laboratory measurements, and would also require incorporating additional geophysical constraints and allowing for other possible contributing factors, such as partial melt, as well as for lateral temperature variations.

The significant spatial variations in the transition zone, with the highest conductivities in areas with significant recent subduction input, suggest that water is carried into the transition zone with the hydrated parts of the lithosphere. This possibility has been previously suggested by a number of studies[10,26]. Water transport into the deep
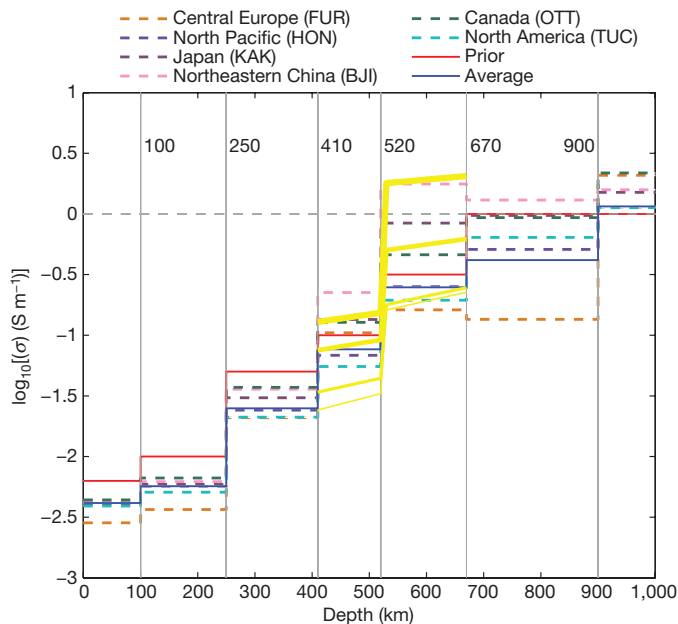
Figure 2 | Global and regional electrical conductivity profiles, based on the three-dimensional inverse solution presented in Fig. 1. The dashed lines correspond to the profiles beneath a set of locations, representative of geographical regions. The blue solid line is the global average. The red solid line represents the prior one-dimensional model used for the inversion[19]. The four yellow lines indicate the existing mineral physics constraints[8] as a function of water content (from the bottom up, in wt%: 0; 0.1, 0.5, 1.0). The three-letter abbreviations refer to the INTERMAGNET geomagnetic observatory codes[27].

mantle is expected to be particularly effective for the cold Pacific plate subducting along the Japan trench, where hydrous phases may remain stable to depths greater than 300 km (ref. 11). Notably this region is associated with particularly high conductivity in our models. The presence of extensive areas of low conductivity, which must be dry, suggests that mechanisms transporting water out of the transition zone must also be active. Further research will be required to clarify the complete transition-zone water cycle.

The model presented here is to our knowledge the first global three-dimensional electrical conductivity model capable of providing constraints on the lateral variations in mantle water content. However, the data set used in this study provides limited vertical and horizontal spatial resolution. The former could be improved by incorporating data from new high quality geomagnetic observatories (especially in the Southern Hemisphere and in Asia) which have now been occupied long enough to provide reliable response functions[27]. Data from satellites such as Champ and Ørsted (and the upcoming SWARM mission) will improve spatial coverage further[28]. Vertical resolution will always be limited by the diffusive nature of electromagnetic fields in a conductor, but could be considerably improved in the upper mantle (including the top of the transition zone) by extending the data set to shorter periods[12]. Interpreting such data will require more sophisticated models for magnetospheric and ionospheric source currents, which are spatially more complex at these periods. More realistic source models would allow more complete use of the available geomagnetic data, including fitting anomalies in all field components[20], and interpreting data from higher geomagnetic latitudes. These extensions will no doubt allow the model presented here to be refined significantly.

METHODS SUMMARY

For our analysis, we use a regularized nonlinear conjugate gradient inversion[12] for global electromagnetic induction studies, based on an adjoint formulation of a staggered-grid finite difference frequency domain numerical solution of Maxwell's equations for spherical geometry[29].

Global observatory response functions from ref. 20 (known as *C* responses[21]) are inverted for conductivity under the assumption that external source fields can be approximated as a zonal dipole[21]. Currents in the auroral ionosphere that are coherent with the magnetospheric equatorial ring current responsible for the dipole source cause this approximation to degrade[20] at geomagnetic latitudes pole-ward of ± 45–$50°$. To minimize artefacts due to these source field complications, responses were corrected for the effect of auroral ionosphere current systems[20], and the inversion was restricted to the 53 observatories equator-ward of $60°$ geomagnetic latitude. The associated jackknife error estimates have median amplitudes of roughly 10%, with larger errors at higher latitudes. The data set is augmented by *C* responses from ref. 21 at six mid-latitude locations to fill in the under-sampled geographical areas.

Coastal observatory responses can be significantly distorted at periods of up to 20 days by the large lateral conductivity contrasts associated with the oceans and underlying sediments. Accurate modelling of these effects requires high numerical resolution (grids of the order of $1° \times 1°$)[30], whereas practicality dictates a much coarser ($10° \times 10°$) grid for the inversions discussed here. To address this issue, we corrected the *C* responses as suggested in ref. 30, using a high resolution ($1° \times 1°$) grid to model near-surface conductive heterogeneities. Tests showed that although fits to some coastal observatories were significantly improved with these corrections, there was little impact on large-scale structure of the resulting conductivity models. This result, and further tests with synthetic data, gives us confidence that even with our approximate treatment this complication does not unduly affect our results.

Full Methods and any associated references are available in the online version of the paper at www.nature.com/nature.

1. Hirth, G. & Kohlstedt, D. L. Water in the oceanic upper mantle: implications for rheology, melt extraction and the evolution of the lithosphere. *Earth Planet. Sci. Lett.* **144**, 93–108 (1996).
2. Dixon, J. E., Dixon, T. H., Bell, D. R. & Malservisi, R. Lateral variation in upper mantle viscosity: role of water. *Earth Planet. Sci. Lett.* **222**, 451–467 (2004).
3. Karato, S.-I. & Jung, H. Water, partial melting and the origin of the seismic low velocity and high attenuation zone in the upper mantle. *Earth Planet. Sci. Lett.* **157**, 193–207 (1998).
4. Williams, Q. & Hemley, R. J. Hydrogen in the deep Earth. *Annu. Rev. Earth Planet. Sci.* **29**, 365–418 (2001).
5. Bercovici, D. & Karato, S.-i. Whole-mantle convection and the transition-zone water filter. *Nature* **425**, 39–44 (2003).
6. Karato, S. The role of hydrogen in the electrical conductivity of the upper mantle. *Nature* **347**, 272–273 (1990).
7. Huang, X., Xu, Y. & Karato, S.-i. Water content in the transition zone from electrical conductivity of wadsleyite and ringwoodite. *Nature* **434**, 746–749 (2005).
8. Yoshino, T., Manthilake, G., Matsuzaki, T. & Katsura, T. Dry mantle transition zone inferred from the conductivity of wadsleyite and ringwoodite. *Nature* **451**, 326–329 (2008).
9. Karato, S. & Dai, L. Comments on "Electrical conductivity of wadsleyite as a function of temperature and water content" by Manthilake *et al. Phys. Earth Planet. Inter.* (in the press).
10. Ohtani, E., Litasov, K., Hosoya, T., Kubo, T. & Kondo, T. Water transport into the deep mantle and formation of a hydrous transition zone. *Phys. Earth Planet. Inter.* **143**, 255–269 (2004).
11. Kawakatsu, H. & Watada, S. Seismic evidence for deep-water transportation in the mantle. *Science* **316**, 1468–1471 (2007).
12. Kelbert, A., Egbert, G. D. & Schultz, A. Non-linear conjugate gradient inversion for global EM induction: resolution studies. *Geophys. J. Int.* **173**, 365–381 (2008).
13. Hae, R., Ohtani, E., Kubo, T., Koyama, T. & Utada, H. Hydrogen diffusivity in wadsleyite and water distribution in the mantle transition zone. *Earth Planet. Sci. Lett.* **243**, 141–148 (2006).
14. Toffelmier, D. A. & Tyburczy, J. A. Electromagnetic detection of a 410-km-deep melt layer in the southwestern United States. *Nature* **447**, 991–994 (2007).
15. Booker, J. R., Favetto, A. & Pomposiello, M. C. Low electrical resistivity associated with plunging of the Nazca flat slab beneath Argentina. *Nature* **429**, 399–403 (2004).
16. Fukao, Y., Koyama, T., Obayashi, M. & Utada, H. Trans-Pacific temperature field in the mantle transition region derived from seismic and electromagnetic tomography. *Earth Planet. Sci. Lett.* **217**, 425–434 (2004).
17. Koyama, T. *et al. Water Content in the Mantle Transition Zone Beneath the North Pacific Derived from the Electrical Conductivity Anomaly* 171–179 (AGU Geophys. Monograph Series 168, 2006).
18. Schultz, A. & Pritchard, G. in *Three Dimensional Electromagnetics* (eds Spies, B. & Oristaglio, V.) 451–476 (Society of Exploration Geophysicists, 1999).
19. Kuvshinov, A. & Olsen, N. A global model of mantle conductivity derived from 5 years of CHAMP, Ørsted, and SAC-C magnetic data. *Geophys. Res. Lett.* **33**, 18301, doi:10.1029/2006GL027083 (2006).
20. Fujii, I. & Schultz, A. The 3D electromagnetic response of the Earth to ring current and auroral oval excitation. *Geophys. J. Int.* **151**, 689–709 (2002).

21. Schultz, A. & Larsen, J. C. On the electrical conductivity of the mid-mantle. 1. Calculation of equivalent scalar magnetotelluric response functions. *Geophys. J. Int.* **88,** 733–761 (1987).
22. Fukao, Y., Widiyantoro, S. & Obayashi, M. Stagnant slabs in the upper and lower mantle transition region. *Rev. Geophys.* **39,** 291–324 (2001).
23. Lawrence, J. F. & Shearer, P. M. Imaging mantle transition zone thickness with *SdS-SS* finite-frequency sensitivity kernels. *Geophys. J. Int.* **174,** 143–158 (2008).
24. Dasgupta, R., Hirschmann, M. M. & Withers, A. C. Deep global cycling of carbon constrained by the solidus of anhydrous, carbonated eclogite under upper mantle conditions. *Earth Planet. Sci. Lett.* **227,** 73–85 (2004).
25. Yoshino, T. & Katsura, T. Effect of iron content on electrical conductivity of ringwoodite, with implications for electrical structure in the transition zone. *Phys. Earth Planet. Inter.* (in the press).
26. Maruyama, S. & Okamoto, K. Water transportation from the subducting slab into the mantle transition zone. *Gondwana Res.* **11,** 148–165 (2007).
27. INTERMAGNET. Participating observatories (map). ⟨http://www.intermagnet.org/Imomap_e.html⟩.
28. Olsen, N. *et al.* CHAOS — a model of the Earth's magnetic field derived from CHAMP, Ørsted, and SAC-C magnetic satellite data. *Geophys. J. Int.* **166,** 67–75 (2006).
29. Uyeshima, M. & Schultz, A. Geomagnetic induction in a heterogeneous sphere: a new three-dimensional forward solver using a conservative staggered-grid finite difference method. *Geophys. J. Int.* **140,** 636–650 (2000).
30. Kuvshinov, A. V., Olsen, N., Avdeev, D. B. & Pankratov, O. V. Electromagnetic induction in the oceans and the anomalous behaviour of coastal C-responses for periods up to 20 days. *Geophys. Res. Lett.* **29,** 1595, doi:10.1029/2001GL014409 (2002).

nature

METHODS

Our model exhibits a general agreement with results from previous deep mantle electromagnetic induction studies. At shallow depths where our data has little sensitivity, that is, in the upper 200 km of the Pacific mantle, there is persuasive evidence for enhanced conductivity due to dissolved hydrogen[31]. The conductivities beneath the central North Pacific have been shown to rise from $0.01\,S\,m^{-1}$ at a depth of 200 km to just over $0.1\,S\,m^{-1}$ at the bottom of the transition zone, then to $1\,S\,m^{-1}$ at about 1,000 km depth[32,33]. These results are consistent with our model at depths ~500 km and below, resolved[12] with the period range of our data (Figs 1, 2). Similar results have been obtained beneath the Canadian Shield[34]. However, conductivities in the transition zone beneath tectonic North America[35] are about half an order of magnitude greater than beneath the Canadian Shield. This location is right at the border between a conductive and a resistive region in our model. Northeastern China has been shown[36] to be at least one order of magnitude more conductive than the central North Pacific, in agreement with our 3D results (Fig. 2). Other profiles[37,38] represent the average between the central North Pacific and the higher conductivity areas resolved by our model (Fig. 1), such as tectonic western North America, northeastern China and Japan. The variability beneath the North Pacific has been explicitly discussed before. For example, Hae *et al.*[13] have estimated that water content variability of 0.03–0.4 wt% would explain electrical conductivity variations in the upper transition zone (400–550 km depth) beneath the Philippine Sea. Although our results for central Europe are consistent with published 1D profiles[39,40], our model shows a steep gradient in this area, with conductivity increasing to the northeast. This feature, which coincides with the Trans European suture zone, has been noted before[41] and may result from lower mantle upwelling[42]. However, further study is required to rule out the possibility of external source contamination at the high geomagnetic latitudes of Northern Europe.

Finally, recent studies of the conductivity of molten carbonates (carbonatites)[43], depleted in Li and rich in Ca, indicate an enhancement in conductivity of three orders of magnitude relative to molten silicates under similar upper mantle conditions. Both geophysical imaging and petrological sampling are consistent with the presence of such highly conducting carbonatites at depths up to ~300 km beneath the East Pacific Rise[43]. However, current evidence suggests carbonates would be unstable at depths relevant to this study, greater than ~400 km (refs 24, 44).

31. Evans, R. L. *et al.* Geophysical evidence from the MELT area for compositional controls on oceanic plates. *Nature* **437**, 249–252 (2005).
32. Lizarralde, D., Chave, A., Hirth, G. & Schultz, A. Northeastern Pacific mantle conductivity profile from long-period magnetotelluric sounding using Hawaii-to-California submarine cable data. *J. Geophys. Res.* **100** (B9), 17837–17854 (1995).
33. Neal, S. L., Mackie, R. L., Larsen, J. C. & Schultz, A. Variations in the electrical conductivity of the upper mantle beneath North America and the Pacific Ocean. *J. Geophys. Res.* **105** (B4), 8229–8242 (2000).
34. Schultz, A., Kurtz, R. D., Chave, A. D. & Jones, A. G. Conductivity discontinuities in the upper-mantle beneath a stable craton. *Geophys. Res. Lett.* **20**, 2941–2944 (1993).
35. Egbert, G. D. & Booker, J. R. Very long period magnetotellurics at Tucson observatory — implications for mantle conductivity. *J. Geophys. Res.* **97**, 15099–15112 (1992).
36. Ichiki, M. *et al.* Upper mantle conductivity structure of the back-arc region beneath northeastern China. *Geophys. Res. Lett.* **28**, 3773–3776 (2001).
37. Utada, H., Koyama, T., Shimizu, H. & Chave, A. D. A. Semi-global reference model for electrical conductivity in the mid-mantle beneath the north Pacific region. *Geophys. Res. Lett.* **30**, 1194–1197 (2003).
38. Kuvshinov, A., Utada, H., Avdeev, D. & Koyama, T. 3-D modelling and analysis of D_{st} C-responses in the North Pacific Ocean region, revisited. *Geophys. J. Int.* **160**, 505–526 (2005).
39. Olsen, N. The electrical conductivity of the mantle beneath Europe derived from C-responses from 3 to 720 hr. *Geophys. J. Int.* **133**, 298–308 (1998).
40. Tarits, P., Hautot, S. & Perrier, F. Water in the mantle: results from electrical conductivity beneath the French Alps. *Geophys. Res. Lett.* **31**, 6612, doi:10.1029/2003GL019277 (2004).
41. Semenov, V. Y. & Jozwiak, W. Lateral variations of the mid-mantle conductance beneath Europe. *Tectonophysics* **416**, 279–288 (2006).
42. Goes, S., Spakman, W. & Bijwaard, H. A lower mantle source for central European volcanism. *Science* **286**, 1928–1931 (1999).
43. Gaillard, F., Malki, M., Iacono-Marziano, G., Pichavant, M. & Scaillet, B. Carbonatite melts and electrical conductivity in the asthenosphere. *Science* **322**, 1363–1365 (2008).
44. Hammouda, T. High-pressure melting of carbonated eclogite and experimental constraints on carbon recycling and storage in the mantle. *Earth Planet. Sci. Lett.* **214**, 357–368 (2003).